THE ASTRONOMICAL JOURNAL, 115:2459–2465, 1998 June


# THE STELLAR POPULATIONS OF PIXELS AND FRAMES

ALVIO RENZINI[1]
European Southern Observatory, Karl-Schwarzschild-Strasse 2, D-85748 Garching bei München, Germany
*Received 1997 October 13; revised 1998 February 11*

## ABSTRACT

Derived from first physical principles, a few simple rules are presented that can help in both the planning and interpretation of CCD and IR-array camera observations of resolvable stellar populations. These rules concern the overall size of the population sampled by a frame as measured by its total luminosity, and allow us to estimate the number of stars (in all evolutionary stages) that are included in the frame. The total luminosity sampled by each pixel (or resolution element) allows us, instead, to estimate the depth to which meaningful stellar photometry can be safely attempted, and below which crowding makes it impossible. Simple relations also give the number of pixels (resolution elements) in the frame that will contain an unresolved blend of two stars of any kind. It is shown that the number of such blends increases quadratically with both the surface brightness of the target and with the angular size of the pixel (or resolution element). A series of examples is presented illustrating how the rules are practically used in concrete observational situations. Application of these tools to existing photometric data for the inner parts of the bulge of M31, M32, and NGC 147 indicates that no solid evidence has yet emerged for the presence of a significant intermediate-age population in these objects.

*Key words:* color-magnitude diagrams — galaxies: individual (M31, M32, NGC 147) — globular clusters: general

## 1. INTRODUCTION

The use of sophisticated software packages for the photometry of stars in crowded fields is now a widespread activity. Routines take a CCD frame and automatically flat-field it; subtract dark, bias, and sky; remove cosmic-ray events; restore bad pixels; and, finally, deliver a catalog of star magnitudes and positions. To some extent, what is left to the astronomer is to plot color-magnitude diagrams, sort out the astrophysical interpretation of them, and, finally, to write the paper. The use of these packages has thus resulted in tremendous progress in the study of resolved stellar populations, including those in Galactic and extragalactic globular clusters, the Magellanic Clouds, the bulges of the Milky Way and M31, the dwarf satellites of M31, and several irregular galaxies in the outskirts of the Local Group and beyond. Such progress has been possible thanks to the large size of the analyzed samples of stellar populations, coupled with superior photometric accuracy. No doubt such achievements would have been impossible with the old, traditional method of direct optical inspection of each stellar image. However, relying entirely on automated procedures can also produce nonsense, and occasionally it actually does so.

We argue that a straightforward application of some basic physical concepts can greatly help the astronomer's work on stellar populations. Some simple tools will be presented that allow one to easily obtain the required numbers for both the efficient use of available telescope facilities and for a deeper understanding of the scientific meaning of the data once they have been obtained.

The paper is organized as follows: Section 2 presents a few basic conceptual tools, whose application to CCD photometry of stellar populations is then illustrated in the following sections. Section 3 deals with the overall size of a sampled stellar population (hence, with the stellar evolutionary phases that can be investigated given such size) and with the size of the stellar population that is sampled by each resolution element (hence, with the depths [limiting magnitude] that can be achieved before crowding effects hamper meaningful stellar photometry). In § 4, several examples are presented to illustrate the practical use of such tools, and § 5 summarizes the main conclusions of this paper.

## 2. NUMBER-LUMINOSITY CONNECTION

In a stellar population of given age, the number $N_j$ of stars in any individual post–main-sequence (PMS) evolutionary stage is clearly proportional to the total bolometric luminosity of the population ($L_T$) and to the duration of the stage ($t_j$), i.e.,

$$N_j = B(t) L_T t_j \, . \qquad (1)$$

The coefficient of proportionality $B(t)$ is the *specific evolutionary flux* of the population (Renzini 1981, 1994; Renzini & Buzzoni 1986; Renzini & Fusi Pecci 1988). It is the number of stars entering or leaving any PMS evolutionary stage per year and per solar luminosity of the population. The product $b(t) = B(t)L_T$ then gives the global rate at which stars leave the main sequence (MS; in stars per year), which is very close to the rate at which stars enter or leave any subsequent evolutionary stage. Thus, $b(t)$ is also a good approximation of the stellar death rate of the population.

The specific evolutionary flux is a very weak function of age, ranging from $\sim 0.5 \times 10^{-11}$ to $\sim 2.2 \times 10^{-11}$ stars $L_\odot^{-1}$ yr$^{-1}$, as age increases from 10 Myr to 15 Gyr, as illustrated in Figure 1. It is also worth noting that the specific evolutionary flux is almost independent of the initial mass function (IMF) of the population. This is because at any age the stars that contribute most of the light span only a very narrow range of masses, around the mass at the MS turnoff, and PMS stars span an even narrower range (see Fig. 1.1 of Renzini 1994).

[1] On leave from the University of Bologna.

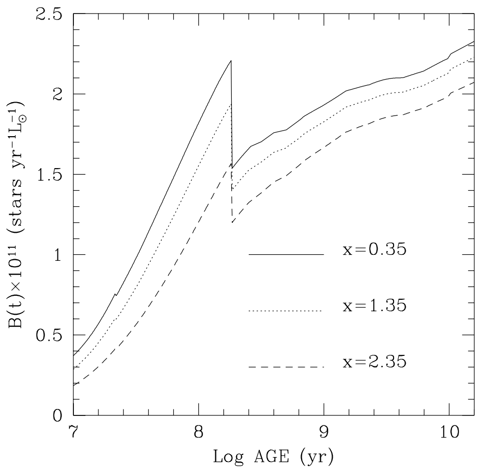


FIG. 1.—Specific evolutionary flux (i.e., the number of stars evolving off the main sequence per year and per unit [solar] luminosity of the parent stellar population) for three values of the slope of the initial mass function, as indicated. The sharp discontinuity at $\sim 10^8$ yr is caused by the appearance of an extended TP-AGB phase.

Of course, this is not the case for the number of stars still on the MS, which is very sensitive to the IMF, $\psi(M) = AM^{-(1+x)}$, especially toward the lower mass limit. The IMF scale factor $A$ establishes the size of the population, hence $A \propto L_T$. With simple algebra one can show that

$$A = B(t) L_T M_{\rm TO}^{1+x} |\dot{M}_{\rm TO}|^{-1} \tag{2}$$

(Renzini 1994), where $M_{\rm TO}(t)$ is the mass of stars at the MS turnoff at age $t$. Figure 2 shows $A/L_T$ as a function of age for a population with solar composition. Note that for a 15 Gyr–old population $A \simeq 1.2 L_T$ and the dependence on the IMF is fairly weak. For such a population the number of MS stars in a given mass interval is then given by

$$dN \simeq 1.2 L_T M^{-(1+x)} dM \ . \tag{3}$$

Finally, one may wish to use the luminosity in a given band rather than the bolometric luminosity, because such a luminosity can be more directly derived from the observations. To this end, one needs *bolometric corrections* for the stellar population, i.e., the quantities $\mathrm{BC}_\lambda$ such that $L_T = \mathrm{BC}_\lambda L_\lambda$. These quantities can be derived theoretically from population synthesis models, or empirically via multiband observations. For the reader's convenience, Figure 2 shows the run with age of such bolometric corrections for three widely used bands ($B$, $V$, and $K$) from the population synthesis models of Maraston (1998). For a solar-metallicity, 15 Gyr–old population, one has

$$L_T \simeq 2.2 L_B \simeq 1.6 L_V \simeq 0.36 L_K \ , \tag{4}$$

which allows the replacement of $L_T$ in equations (1)–(3). The same coefficients in the models of Buzzoni (1989) have the values 2.5, 2.1, and 0.43, respectively. In summary, equation (1) allows the estimation of the number of stars in each PMS phase, while an integration of the IMF with the scale factor given by equation (2) gives the number of MS stars.

## 3. POPULATION SAMPLING

Several very useful consequences follow from the simple fact that the number of stars in a given phase is proportional to the sampled luminosity. A straightforward application of equations (1)–(3) can indeed tell a great deal about the astrophysical information that can be extracted from a given observation.

### 3.1. *Stellar Population of a CCD Frame*

There are two ways to estimate the sampled luminosity. The first, especially useful for planning observations, relies on surface brightness information available in the literature.

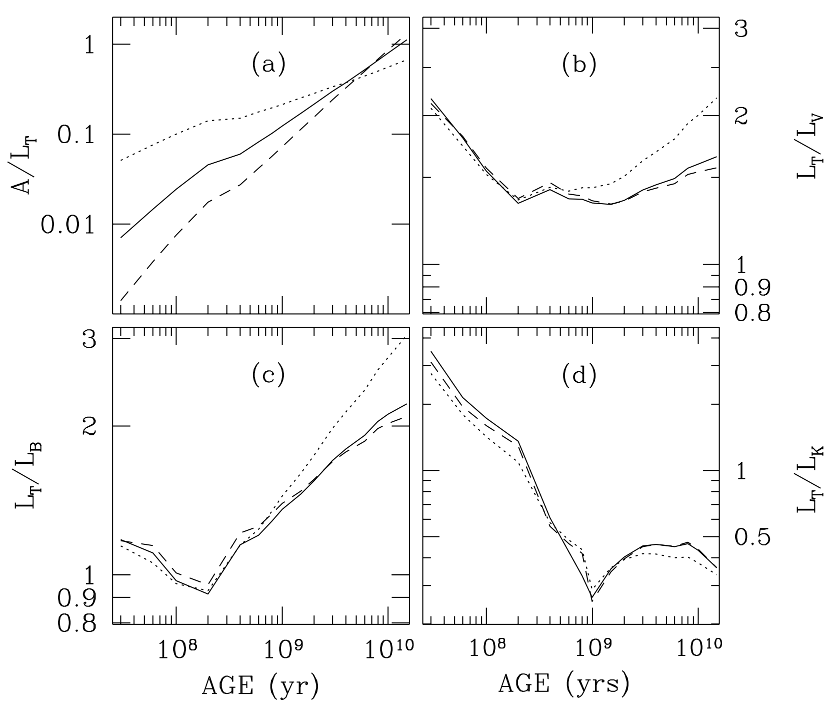


FIG. 2.—(*a*) Ratio of the scale factor $A$ of the IMF to the total bolometric luminosity of a stellar population as a function of its age. (*b*) Ratio of the bolometric luminosity to the $V$-band luminosity as a function of age for a solar-metallicity population. (*c*) Same as (*b*), but for the $B$-band luminosity. (*d*) Same as (*b*), but for the $K$-band luminosity.

Suppose the CCD camera has a field of view of $F_{\rm oV}$ arcsec$^2$, and let the surface brightness, extinction, and true distance modulus of the object be $\mu_\lambda$ mag arcsec$^{-2}$, $A_\lambda$ mag, and "mod," respectively. The sampled luminosity is therefore

$$L_T = {\rm BC}_\lambda F_{\rm oV}\, 10^{-0.4(\mu_\lambda - A_\lambda - {\rm mod} - M_{\lambda,\odot})}\,, \quad (5)$$

where $M_{\lambda,\odot}$ is the absolute magnitude of the Sun in the $\lambda$ band.

The second method makes use of the obtained data. Once the CCD frame has been dark-, bias-, and sky-subtracted, flat-fielded, calibrated, and cosmic-ray–removed, then the total number of counts in the whole frame (the sum of the values of all the pixels) can be immediately translated into an apparent integrated magnitude of the whole frame. Hence, applying extinction and distance corrections, one gets the total luminosity sampled by the frame in a given band. The only steps that require some care are the sky subtraction and saturated images. Obvious precautions include measuring the sky well outside the object, removing bright interlopers, and using shallow frames without saturated images. Getting the sampled luminosity in this way should be done routinely, for this is the most correct and straightforward way to estimate $L_T$, and this quantity is of great utility for the science to be done with the data.

For the sake of concreteness, let us suppose that the camera samples a luminosity $L_T = 10^5\ L_\odot$, and that the stellar population is $\sim$15 Gyr old and of near-solar metallicity. Table 1 then gives the number of stars in each of a series of representative evolutionary phases. For the MS, the number of stars is obtained by integrating the IMF from the hydrogen burning limit at $M_{\rm inf} = 0.1\ M_\odot$ to the MS turnoff at $M_{\rm TO} = 0.9\ M_\odot$, and using equation (3). For example, assuming a single-slope Salpeter IMF,

$$N_{\rm MS} = 1.2 L_T \int_{0.1}^{0.9} M^{-2.35}\, dM \simeq 19\left(\frac{L_T}{1\ L_\odot}\right). \quad (6)$$

The other entries in Table 1 include the subgiant branch (SGB), with stars from the MS turnoff to the base of the red giant branch (RGB); the RGB itself, which ends with helium ignition at the RGB tip (RGBT); RGB stars within 1 mag of the RGBT; the horizontal branch (HB); the early asymptotic giant branch (E-AGB); the thermally pulsing AGB (TP-AGB); the long-period variable (LPV) phase; the post-AGB (P-AGB) phase, from the AGB tip down to a luminosity 10 times lower; the planetary nebula (PN) phase; the white dwarf phase, from the end of the P-AGB phase down to a luminosity $\sim 10^{-3}\ L_\odot$; the blue stragglers (BS); and, finally, the TP-AGB progeny of BSs (BS-TP-AGB). The LPVs are likely to be in the TP-AGB phase. They are not found in metal-poor globular clusters of our Galaxy; they are found instead in the old metal-rich globulars that belong to the Galactic bulge, where they can reach $M_{\rm bol} \simeq -5.0$ (Frogel & Elias 1988; Guarnieri, Renzini, & Ortolani 1997). It is worth emphasizing that only objects brighter than this limit could be indicative of an intermediate-age population. Lifetimes in the various phases are derived from tested evolutionary models (e.g., Renzini & Fusi Pecci 1988). Equation (1) is used for all phases except for MS, TP-AGB, BS, and BS-TP-AGB. For the MS phase, equation (6) is used. The $10^6$ yr lifetime for the TP-AGB phase is likely to be an overestimate for a 15 Gyr–old population (see Renzini & Fusi Pecci 1988). BSs are a trace population of merged binaries, and their number-to-luminosity conversion must be established empirically. For this purpose, the globular cluster M3 was used (Renzini & Fusi Pecci 1988), while for the BS-TP-AGB phase, the recipe given by Renzini & Greggio (1990) was adopted.

TABLE 1

STAR NUMBERS FOR $L_T = 10^5\ L_\odot$, AGE 15 Gyr, AND $Z = 1\ Z_\odot$

| Evolutionary Phase | $t_j$ (yr) | $N_j$ |
|---|---|---|
| MS | $>10^{10}$ | $1.9 \times 10^6$ |
| SGB | $3 \times 10^9$ | 6000 |
| RGB | $6 \times 10^8$ | 1200 |
| RGBT | $5 \times 10^6$ | 10 |
| HB | $10^8$ | 200 |
| E-AGB | $1.5 \times 10^7$ | 30 |
| TP-AGB | $10^6$ | 2 |
| LPV | $2.5 \times 10^5$ | 0.5 |
| P-AGB | $3 \times 10^5$ | 0.6 |
| PN | $2.5 \times 10^3$ | 0.005 |
| WD | $10^9$ | 2000 |
| BS | $2 \times 10^9$ | 200 |
| BS-TP-AGB | $10^6$ | 0.06 |

Table 1 illustrates that for the given size of the population ($10^5\ L_\odot$) several evolutionary phases are well represented, while for others the number of stars is very scarce. When such a number is smaller than unity, it can be used as the probability to find a star of a given kind in the frame. For example, with $L_T = 10^5\ L_\odot$, the probability of finding a planetary nebula in the frame is only $\sim$0.5%, and hence a luminosity $\sim 2 \times 10^7\ L_\odot$ should be explored in order to have a reasonable chance to find one PN, in practice, among the whole globular cluster family of a galaxy like the Milky Way.

Therefore, Table 1 together with the simple relations given above can be used to tailor the observations in order to collect the appropriate number of stars in particular evolutionary phases, depending on the science goals of any specific project. Indeed, for any kind of stellar system one can choose to point the telescope at a region where the surface brightness is appropriate and, hence, the luminosity sampled by the camera has the adequate size for the specific science project. Equation (1) can also be used in the reverse direction, i.e., to infer the duration of a specific evolutionary phase from the observed number of stars in the phase and from the sampled luminosity. For example, the duration of the LPV phase in metal-rich globular clusters was derived in this way (Renzini 1993).

### 3.2. *Stellar Population of a Pixel*

To sample an adequate number of stars, one may be tempted to observe a field in the central region of an object, where the surface brightness and sampled luminosity are highest. However, by moving to high surface brightness regions crowding will inevitably degrade the photometric accuracy, and meaningful stellar photometry may even become impossible. Clearly, an optimization is required, finding a compromise between the conflicting needs of securing an adequate size for the sampled population and of accurate photometry of the stars to be measured. The effects of crowding will depend on the specific code that is adopted, with some codes being better than others. However, a great deal about the effects of crowding can be understood *from first principles.*

Having determined the luminosity $L_T$ sampled by the whole CCD (or IR-array) frame, one can easily derive the average luminosity $L_T^{\rm pix}$ sampled by each pixel:

$$L_T^{\rm pix} = L_T/N^{\rm pix} , \quad (7)$$

where $N^{\rm pix}$ is the number of pixels in the detector. The actual resolution element will generally exceed the size of 1 pixel, and in the case of ground-based observations, it will depend on seeing. The luminosity sampled by one resolution element is then the product of $L_T^{\rm pix}$ times the number of pixels in each resolution element. In what follows, the term *pixel* will be used for short, but everything said for pixels would apply equally well to the actual resolution elements.

Crowding has two main effects on the results of automatic reductions of CCD frames by photometric packages. One obvious effect is the reduced photometric accuracy: the fit to the stellar point-spread function (PSF) is degraded by the presence of neighboring stars, and the error in magnitudes exceeds that expected from the pure Poisson photon noise. The less obvious effect is that occasionally two (or more) stars fall on the same pixel, and the package is not able to realize the multiple nature of the object that is then mistaken as a single star. The former effect results in broadened color-magnitude diagrams and smeared luminosity functions, but one can easily learn how to handle such reduced photometric accuracy. The latter effect is much more insidious, as it generates false stars that do not have counterparts in the real population but may resemble objects with the attractive characteristics that one wishes to find.

Let $N_j = B(t)L_T^{\rm pix} t_j$ be the number of stars in phase $j$ per pixel; for $N_j < 1$, this is also close to the probability that a pixel contains one star in phase $j$. Hence, the probability that a pixel contains two such stars is $\sim N_j^2$, and the number $N_{2j}$ of such events in the whole frame is

$$N_{2j} = N_j^2 N^{\rm pix} = [B(t)L_T^{\rm pix} t_j]^2 N^{\rm pix} = [B(t)L_T t_j]^2/N^{\rm pix} . \quad (8)$$

Since $L_T$ is proportional to the surface brightness sampled by the camera, one sees that the number of $2j$-star blends is proportional to the square of the surface brightness expressed in physical units ($L_\odot$ arcsec$^{-2}$). This *square law* can be easily generalized to any kind of star pair (e.g., the blend of a WD and an MS star), with the number $N_{jk}$ of such $jk$ blends in the frame being

$$N_{jk} = N_j N_k N^{\rm pix} = [B(t)L_T]^2 t_j t_k/N^{\rm pix} , \quad (9)$$

where the second equality applies only to PMS pairs. Hence, the number of any kind of two-star blend in the frame varies as the square of the surface brightness of the target. Moreover, the number of triplets varies with the cube of the surface brightness, that of quartets with the fourth power, and so on.

This square law uncovers yet another insidious effect of crowding. The surface brightness of stellar systems can be very high at the center, and then fall rapidly toward the outer regions. Therefore, the number of star pairs sharing the same pixel will increase toward the center as the square of the surface brightness, i.e., the "exceptional" stars will appear much more centrally concentrated than the underlying light distribution. One may be tempted to conclude, for instance, that the exceptional stars were produced by a recent burst of star formation that took place in the central regions—a plausible hypothesis that may become a wishful finding. From equation (9) it follows that the number $N_{jk}$ of $jk$ blends is also proportional to the square of the actual resolution.

A safe criterion for accurate photometry states that meaningful magnitudes can be obtained only for stars much brighter than $L_T^{\rm pix}$, i.e., for $L \gg L_T^{\rm pix}$. By contrast, there is no way to extract meaningful information on individual stars fainter than this limit, i.e., for $L \lesssim L_T^{\rm pix}$. When this applies even to the brightest stars in the population, one enters the domain of the surface brightness fluctuation method (Tonry & Schneider 1988), and one had better leave photometric packages aside: the frame is *burned out*, almost like an overexposed photographic plate.

Of course, the quality of the photometry degrades in a continuous fashion as the $L_T^{\rm pix}$ limit is approached. For example, suppose that in a given frame the photometry of the brightest stars is on the safe side of the criterion. Progressing to fainter objects, photometry will become more and more hazardous as their luminosity approaches $L_T^{\rm pix}$. Along with real individual stars, a photometric package will deliver an increasing number of $jk$ pairs in the same magnitude interval. When working on such a mined terrain, equation (9) can be used to estimate the number of contaminants, and it would not be wise to trust the output of a photometric package when the estimated number of contaminants in a given magnitude bin becomes a sizable fraction of the total star counts in the bin.

This criterion for safe photometry can be made even more effective if assisted by appropriate simulations and numerical experiments: for example, comparing the results of running a given photometric package on a full-resolution frame, and then on the same frame with the resolution having being artificially degraded (see, e.g., DePoy et al. 1993). Indeed, the ability to resolve blends into individual components is code dependent, while the (photon) signal-to-noise ratio (S/N) will also affect the output. In essence, a modest effort invested in such simulations would *calibrate* the criterion, allowing it to predict with greater accuracy the performance of a specific photometric package.

## 4. SOME EXAMPLES

A few concrete examples are presented to illustrate the use and effectiveness of the tools described in the previous sections. These examples include the extreme cases one is interested in at either the top or the bottom end of the luminosity function, and involve both the frame- and pixel-sampling criteria. These examples are restricted to the case of an old stellar population, but the tools provided in this paper should be applicable to populations of any age distribution.

### 4.1. *Brightest Stars in the Bulge and Satellites of M31*

The red giant (RGB + AGB) luminosity function in nearby galactic spheroids can, in principle, be used to infer whether an intermediate-age population is present in such objects, implying a population significantly younger than Galactic globular clusters. However, the presence of objects apparently brighter than the RGB tip ($M_{\rm bol} \simeq -3.8$ for [Fe/H] $\simeq 0$) cannot be interpreted as evidence for an intermediate-age population, unless their number is significantly in excess of that of LPVs found in old, near–solar-metallicity globular clusters, where LPVs extend up to

$M_{\rm bol} \simeq -5.0$. A trace population of AGB stars even brighter than this limit is represented by the progeny of blue stragglers, a minority component in old stellar systems. Finally, under extreme crowding conditions, apparently bright objects may actually be the result of unresolved blends.

Table 2 reports sampling information for various locations in the bulge of M31, and in M32 and NGC 147, assuming a common distance modulus of 24.4 mag. The sampled blue and bolometric luminosities per square arcsecond ($L_B$ and $L_T$) take into account the extinction correction assuming $E(B-V) = 0.18$ (hence $A_B = 0.756$; Han et al. 1997), and adopting $L_T = 2.5L_B$. The extinction correction accounts for the factor of 2 difference in some of the numbers with respect to Table 1 in Renzini (1993). The last column in Table 2 gives the number of pixels containing two RGB stars within 1 mag from the RGB tip, for specific values of the size of the resolution element (see below). The majority of these events will produce artifact "stars" brighter than the RGB tip, which might be mistaken for bright AGB stars.

The first M31 row in Table 2 refers to the central 4″ of M31, an area that was observed by Davidge et al. (1997) with an adaptive optics device with a pixel size of 0″.0343 that—using one of the two M31 nuclei as a reference star—allows a resolution of 0″.14 (FWHM). The surface brightness in the field drops from $\mu_B \simeq 13.8$ mag arcsec$^{-2}$ at the center to $\sim 16.7$ at the edge of the observed field (Schweizer 1979). Taking into account the square-law effect (§ 3.2), a surface brightness $\mu_B \simeq 15$ mag arcsec$^{-2}$ can be taken as representative of the field. Thus, each pixel collects $\sim 4500\ L_\odot$ and each resolution element $\sim 7.5 \times 10^4\ L_\odot$, comparable to that of a typical globular cluster. The actual population of each resolution element can be obtained by scaling from Table 1, multiplying the last column by 0.75. In particular, each resolution element contains $\sim 0.4$ LPVs and $\sim 6.5$ RGBT stars. No meaningful stellar photometry can be extracted from such a frame, and the apparent "bright AGB stars" reported by Davidge et al. must merely be peaks caused by the stochastic fluctuation in the number of LPV and RGB stars per resolution element. *Hubble Space Telescope* (*HST*) images of this central field could be used both to obtain an accurate surface brightness distribution and to attempt the resolution into individual components of at least some of the apparently brightest objects.

Moving to less crowded fields, let us suppose we observe at 2′ from the center of M31 with the NIC2 camera on *HST*. With a pixel size of 0″.06 and a field of view of 19″.2 × 19″.2, NIC2 would sample a total luminosity of $\sim 1.7 \times 10^7\ L_\odot$, or $\sim 160\ L_\odot$ pixel$^{-1}$. Scaling from Table 1, one infers that the NIC2 frame should include $\sim 80$ LPVs. From equation (8) one obtains that $\sim 20$ two–RGBT star events in 1 pixel should also be present in the frame (cf. Table 2). As also reported in Table 2, one sees that at 4′ from the center, the number of two-RGBT blends has decreased by a factor of 10, while the number of LPVs decreases by a factor of 3, an illustration of the "square law" mentioned in § 3.2. When taking into account that the actual resolution will be a few times worse than 1 pixel, one can conclude that NIC2 will barely be able to obtain meaningful stellar photometry in M31 closer than $\sim 2'$ from the center.

The 2′ and 4′ M31 fields were also observed by Rich & Mould (1991) and Rich, Mould, & Graham (1993) with $\sim 1$ arcsec$^2$ resolution. One expects that in both fields two-RGBT blends are more numerous than LPVs (Renzini 1993; see also DePoy et al. 1993 for detailed simulations). A better resolution is clearly required, and Rich & Mighell (1995) used pre-COSTAR *HST* Wide Field Camera data in an attempt to improve upon previous ground-based observations. The sharp core and extended wings of the aberrated PSF forced them to abandon the PSF-fitting technique in the very crowded central and 2′ fields they observed, and tailor to the nature of the data an aperture photometry approach. In the central field their 0″.4 aperture samples an average $\sim 10^4\ L_\odot$, and hence photometry of stars of comparable luminosity must be very uncertain. Indeed, Rich & Mighell admit that they "cannot be *certain* that stars brighter than $I = 19.5$ [corresponding to $M_{\rm bol} = -4.5$] are intrinsically luminous or accidentally measured bright due to photometric errors." The rather blue $R-I$ color of the detected objects also favors the bright events' being blends of RGB (or LPV + RGB) stars, rather than extended AGB objects that would be rather red. In conclusion, NIC2 offers our best hope to check whether or not the bulge of M31 harbors an extended AGB made of intermediate-age stars, and yet this will be possible only beyond some arcminutes from the center.

Several studies have focused on M32, the dwarf elliptical satellite of M31. Table 2 shows that the two innermost fields are too crowded for reliable stellar photometry with the resolution available to Davidge & Nieto (1992), each resolution element being $\sim 0.16$ arcsec$^2$. The situation was far better for the outer field located at 2′ from the center, which was observed from the ground by Freedman (1992) with $\sim 0.3$ arcsec$^2$ resolution elements. With the average surface brightness quoted by Freedman ($\mu_V = 21$, or $\mu_B = 21.9$) over a field of view of 4000 arcsec$^2$, one expects $\sim 130$ LPVs and $\sim (0.3 \times 0.7)^2 4000/0.3 \approx 600$ two-RGBT blends in the frame. By contrast, Freedman detected only $\sim 100$ stars brighter than the RGB tip. However, the *average* surface brightness of this field may actually be significantly lower than mentioned by Freedman. From Peletier (1993) the much lower *local* value $\mu_B = 24.6$ can be inferred at the 2′ position (Renzini 1993), a value also reported in Table 2. Assuming this local value to be representative of the average over the actual field of view, one obtains a $\sim 10$ times lower value of $N_{\rm LPV}$ and a $\sim 100$ times lower value of $N_{\rm 2RGBT}$. The apparent discrepancy is at least in part a result of the strong $\mu_B$-gradient across the field; hence, to estimate of the number of blends one should take into account the actual surface brightness distribution within the $\sim 1'$ field of view. It appears that the issue has been resolved by recent observations with *HST* Wide Field Planetary Camera 2 (WFPC2) at 1′–2′ from the center of M32, which did not reveal the presence of AGB stars so (bolometrically) bright to be indicative of an intermediate-age component (Grillmair et al. 1996). Grillmair et al. conclude that the optically bright objects seen in previous ground-based work were artifacts of crowding.

*HST* observations of another satellite of M31, NGC 147, have revealed the presence of a population of stars up to $\sim 1$ mag brighter in $I$ than the RGB tip (Han et al. 1997). The Han et al. inner field is centered on the nucleus of NGC 147, and extends to $\sim 100''$ from the center along the major axis. From Table 2 one sees that at the very center of NGC 147 the surface brightness is still low enough for accurate photometry to be done to rather faint luminosities. With an 0″.1 pixel size, each WFPC2 pixel will sample $\sim 43\ L_\odot$, and

TABLE 2

STELLAR POPULATION SAMPLING IN THE BULGE AND SATELLITES OF M31

| $r$ | $\mu_B$ (mag arcsec$^{-2}$) | $L_B$ ($L_\odot$ arcsec$^{-2}$) | $L_T$ ($L_\odot$ arcsec$^{-2}$) | $N_{\rm LPV}$ (stars arcsec$^{-2}$) | $N_{\rm RGBT}$ (stars arcsec$^{-2}$) | $N_{\rm 2RGBT}$ (events) |
|---|---|---|---|---|---|---|
| M31 bulge: | | | | | | |
| 0″–4″…… | 15 | $1.5 \times 10^6$ | $3.8 \times 10^6$ | 20 | 410 | … |
| 2′………. | 19.8 | $1.8 \times 10^4$ | $4.5 \times 10^4$ | 0.24 | 4.9 | 21 |
| 4′………. | 21 | $6.0 \times 10^3$ | $1.5 \times 10^4$ | 0.06 | 1.6 | 2 |
| 11′.5 ……. | 23 | $9.5 \times 10^2$ | $2.4 \times 10^3$ | 0.01 | 0.2 | … |
| M32: | | | | | | |
| 5″ ……… | 17 | $2.4 \times 10^5$ | $6.0 \times 10^5$ | 3 | 66 | … |
| 27″ …….. | 18 | $9.6 \times 10^4$ | $2.3 \times 10^5$ | 1.2 | 23 | … |
| 2′………. | 21.9 | $2.6 \times 10^3$ | $6.5 \times 10^3$ | 0.03 | 0.7 | 600 |
| 2′………. | 24.6 | $2.2 \times 10^2$ | $5.5 \times 10^2$ | 0.003 | 0.06 | 6 |
| NGC 147: | | | | | | |
| 0″.0 …….. | 22.55 | $1.4 \times 10^3$ | $4.3 \times 10^3$ | 0.02 | 0.4 | … |

serious crowding problems will be encountered more or less at the level of the HB. Therefore, image blends can be excluded as the origin of the extended AGB in this galaxy.

The NGC 147 integrated magnitude within the $r = 100''$ isophote is $B_0 \simeq 10.6$ (Hodge 1976), and the total blue luminosity sampled by WFPC2 on the inner field is roughly $L_B \simeq 5 \times 10^7\ L_\odot$, or $L_T \simeq 1.25 \times 10^8\ L_\odot$. This may somewhat overestimate the actual luminosity sampled within the stealthy perimeter of the WFPC2 field of view, so $\sim 10^8\ L_\odot$ seems to be a more conservative estimate. (The luminosity actually sampled by WFPC2 could be obtained as described in § 3.1.) Scaling from Table 1 one then expects $\sim 500 \pm 250$ LPVs to lie above the RGB tip, while Han et al find $\sim 250$ such stars. The large statistical uncertainty comes from the estimated LPV lifetime being based on 4 ($\pm 2$) LPVs in 47 Tuc. The average metallicity of NGC 147 ([Fe/H] $= -0.9$) is close to that of 47 Tuc ($-0.7$), yet because of the large metallicity dispersion only a fraction of the stellar population is expected to exceed the metallicity threshold ([Fe/H] $\gtrsim -1$) above which Galactic globular clusters harbor LPVs (Frogel & Elias 1988). Finally, scaling from Table 1 one expects to find $\sim 75$ TP-AGB stars being the progeny of BSs, hence reaching brighter luminosities on the AGB than the bulk population of single stars.

In conclusion, a population of LPVs similar to the ones in old, metal-rich globular clusters such as 47 Tuc appears able to account for the extended AGB of NGC 147 without appealing to an intermediate-age population. The gradient in the frequency of bright AGB stars can well result from the higher proportion of metal-rich stars near the center that was found by Han et al., rather than from a recent burst of star formation. The above discussion has also indicated that crowding has so far seriously limited the photometry of individual stars in the inner regions of M32 and the bulge of M31, while high-resolution *HST* imaging of an outer field in M32 has failed to detect an extended AGB. From all this it appears that no compelling evidence has yet emerged for the presence of a major intermediate-age component in any of these systems.

### 4.2. *Main-Sequence Turnoff of the M31 Bulge*

As is well known, the best way of determining the age of a stellar population, or to detect an unequivocal age spread, is to directly access the main-sequence turnoff. Experience has shown that photometry should reach at least 2 mag below the turnoff with S/N $\gtrsim 10$ in order to determine the turnoff magnitude with adequate accuracy (say, $\sim 0.1$ mag, corresponding to a $\sim 10\%$ error in age).

With $M_V^{\rm TO} \simeq 5$, as appropriate for a metal-rich population 15 Gyr old, the turnoff is to be found at $V \simeq 29.4$, and therefore one should reach $V \simeq 31.4$ with the appropriate S/N. This seems to be out of reach even for a heroic effort with *HST*. The proposed Next Generation Space Telescope (NGST) instead will have a collecting area and quantum efficiency adequate to reach this limit, but let us consider the crowding problem.

For this example let us focus on the outermost of the M31 fields in Table 2, which corresponds to a projected distance of $\sim 2$ kpc from the center, in fact near the edge of the bulge. With an absolute bolometric surface brightness of $\sim 2400\ L_\odot$ arcsec$^{-2}$, each 0″.06 pixel of the NGST near-IR camera (Stockman 1997, p. 84) will sample $\sim 8.6\ L_\odot$. Two magnitudes below turnoff corresponds to stars of $\sim 0.7\ M_\odot$, assuming the turnoff itself is at $0.9\ M_\odot$. Hence, integrating the IMF following the equation (3) prescription, one finds that on average each pixel will contain $\sim 3.6$ stars brighter than $V = 31.4$. It appears that the main-sequence turnoff of the M31 bulge will be out of reach as a result of crowding, even with NGST. A resolution some 10 times better (i.e., $\sim 0''.005$) would be needed, something that would require a baseline of $\sim 80$ m, either with an interferometer, or with a single dish.

### 4.3. *Bottom of the Main Sequence in the Galactic Bulge*

The determination of the IMF of the Galactic bulge is of great astrophysical interest. It represents a unique chance of measuring directly the lower IMF of an old, metal-rich population that may have formed in a major starburst some 15 Gyr ago. Moreover, knowing the IMF of the bulge would be of great help in interpreting the results of the various microlensing experiments now underway.

This example focuses on a bulge field $\sim 6°$ south of the Galactic center. With a surface brightness $\mu_{V,0} = 19.7$ mag arcsec$^{-2}$ (corrected for extinction) and a true distance modulus of 14.5 mag, the absolute surface brightness is $M_{V,0} = 5.2$ mag arcsec$^{-2}$, or 1.5 bolometric $L_\odot$ arcsec$^{-2}$, using $L_T = 2.1 L_V$. Among currently available telescopes and cameras, NICMOS on *HST* offers the best chance of reaching the bottom of the main sequence. With a field of view of 19″.2, the NIC2 camera will sample $\sim 420\ L_\odot$, and following equation (6) the frame will include $\sim 8000$ stars. With $256^2$ pixels, there will be on average $\sim 8$ pixels available for each star, and it may turn out to be very difficult to do accurate photometry down to the hydrogen burning limit. However, this assumes a Salpeter IMF slope ($x = 1.35$) all the way down to $\sim 0.1\ M_\odot$. If the IMF of the bulge flattens out below 0.6 $M_{\odot}$, as it does in the solar neighborhood (Gould, Bahcall, & Flynn 1997), then one expects to find $\sim 10$ times fewer stars in the frame, and there will be over 100 pixels available for each stellar image. This seems to be perfectly adequate for accurate photometry down to the MS limit, provided the integration time is long enough. However, given the strong surface brightness gradient, it appears difficult to obtain complete IMF information for fields somewhat closer to the Galactic center.

## 5. CONCLUSIONS

Simple tools have been presented that may help the astronomer wishing to extract as much sound science as possible from CCD/IR-array data on stellar populations. The main conclusions of this paper may be summarized as follows:

1. While planning CCD/IR-array observations of stellar populations in globular clusters, in the Galactic bulge, or in nearby resolvable galaxies, the total luminosity sampled by the frame (in units of $L_{\odot}$) should be estimated from the known surface brightness distribution of the target objects.
2. On the basis of this "frame luminosity," the luminosity sampled by each pixel of the camera (or by each expected resolution element) should also be evaluated.
3. On the basis of the frame luminosity, the astronomer can estimate with very good accuracy the number of stars in each evolutionary phase that will be framed by the camera, thus allowing a decision as to whether the sampling is statistically adequate for the specific evolutionary phases under investigation.
4. On the basis of the "pixel luminosity," the astronomer can estimate with very good accuracy down to which magnitude one can trust the result of individual star photometry as performed by current photometric packages.
5. Frame sampling and pixel sampling set conflicting requirements, the former demanding observation of regions of high surface brightness (in order to secure a statistically adequate sample of stars), and the latter requiring observation of regions of low surface brightness (in order to secure reliable photometry of individual stars). The tools provided in this paper allow the astronomer to proceed very rapidly with the necessary optimization, or to conclude that a certain scientific goal is not reachable with the available technology.
6. After the data have been taken, the frame luminosity should be estimated directly from the frame itself, after the frame has been properly dark-, bias-, and sky-subtracted and calibrated. This will provide the most accurate estimate of both the frame and pixel luminosity as possible.
7. A basic criterion for the limit imposed by crowding states that reliable photometry can be obtained only for those stars that are brighter than the average luminosity sampled by each pixel (resolution element). Experiments that are easy to imagine should allow one to more finely calibrate this criterion, establishing in a quantitative way—and for any specific photometric package—how the photometry of individual stars degrades as this limit is approached, and to what extent star counts in a given magnitude bin are contaminated by blends of stars in fainter magnitude bins.
8. Some straightforward checks should be made when photometric packages restitute exceptionally bright objects, in order to ascertain whether they are real stars rather than the result of accidental blends of fainter stars sharing the same resolution element. This second option should be carefully evaluated, especially when the surface density of such objects appears to be roughly proportional to the square power of the surface brightness.
9. The *artificial star* experiments as currently performed by standard photometric packages may be adequate to estimate the completeness of star counts as a function of magnitude. However, they would require the repetition of the experiment nearly as many times as the number of stars in the frame, in order to assess the extent of the *migration* of a fraction of stars toward brighter magnitudes because of blending with other stars.
10. An application of these tools to existing photometric data for the bulge of M31, M32, and NGC 147 indicates that no solid evidence has yet emerged for the presence of an intermediate-age population in these objects.

I wish to thank Mike Rich for extensive discussions—over the last several years—on the effects of crowding on the results of package photometry of Local Group galaxies. I wish also to thank Russell Cannon for a critical reading of the manuscript that resulted in an improved presentation. I am grateful to Claudia Maraston for her help in producing Figure 2.

## REFERENCES

Buzzoni, A. 1989, ApJS, 71, 817
Davidge, T. J., & Nieto, J.-L. 1992, ApJ, 391, L13
Davidge, T. J., Rigaut, F., Doyon, R., & Crampton, D. 1997, AJ, 113, 2094
DePoy, D. L., Terndrup, D. M., Frogel, J. A., Atwood, B., & Blum, R. 1993, AJ, 105, 2121
Freedman, W. L. 1992, AJ, 104, 1349
Frogel, J. A., & Elias, J. H. 1988, ApJ, 324, 823
Gould, A., Bahcall, J., & Flynn, C. 1997, ApJ, 482, 913
Grillmair, C. J., et al. 1996, AJ, 112, 1975
Guarnieri, M. D., Renzini, A., & Ortolani, S. 1997, ApJ, 477, L21
Han, M., et al. 1997, AJ, 113, 1001
Hodge, P. W. 1976, AJ, 81, 25
Maraston, C. 1998, MNRAS, in press
Peletier, R. F. 1993, A&A, 271, 51
Renzini, A. 1981, Ann. Phys., 6, 87
———. 1993, in IAU Symp. 153, Galactic Bulges, ed. H. Dejonghe & H. J. Habing (Dordrecht: Kluwer), 151
Renzini, A. 1994, in Galaxy Formation, ed. J. Silk & N. Vittorio (Amsterdam: North Holland), 303
Renzini, A., & Buzzoni, A. 1986, in Spectral Evolution of Galaxies, ed. C. Chiosi & A. Renzini (Dordrecht: Reidel), 135
Renzini, A., & Fusi Pecci, F. 1988, ARA&A, 26, 199
Renzini, A., & Greggio, L. 1990, in Bulges of Galaxies, ed. B. J. Jarvis & D. M. Terndrup (Garching: ESO), 47
Rich, R. M., & Mighell, K. J. 1995, ApJ, 439, 145
Rich, R. M., & Mould, J. R. 1991, AJ, 101, 1286
Rich, R. M., Mould, J. R., & Graham, J. R. 1993, AJ, 106, 2252
Schweizer, F. 1979, ApJ, 233, 23
Stockman, H. S. 1997, The Next Generation Space Telescope (Washington: AURA, Inc.)
Tonry, J. L., & Schneider, D. P. 1988, AJ, 96, 807